THE PENNSYLVANIA STATE UNIVERSITY
SCHREYER HONORS COLLEGE

DEPARTMENT OF CIVIL AND ENVIRONMENTAL ENGINEERING

THE QUANTIFICATION OF MORINGA PROTEIN AND MODELING OF THE F-SAND COLUMN

KATHLEEN LAUSER
SPRING 2015

A thesis
submitted in partial fulfillment
of the requirements
for a baccalaureate degree
in Chemical Engineering
with honors in Environmental Engineering

Reviewed and approved* by the following:

Stephanie Velegol
Instructor, Civil and Environmental Engineering
Thesis Supervisor

Eric Donnell
Associate Professor, Civil and Environmental Engineering
Honors Adviser

* Signatures are on file in the Schreyer Honors College.

ABSTRACT

Seeds from the *Moringa oleifera* tree have been used for centuries to purify water. Using the purifying ability of Moringa seeds, we have created a special sand filter called f-sand to address the scarcity of clean water in developing countries. F-sand is created by absorbing an antimicrobial, cationic protein (MOCP) from *Moringa oliefera* seeds onto sand particles. Because of its positive charge, f-sand can attract and capture negatively charged particles and microbes to purify water. It is our goal for these f-sand filters to be utilized in the developing world. Before that can be accomplished, further study is necessary both on the MOCP levels in these seeds and the effectiveness of the f-sand filters upon scale-up.

One major concern with Moringa water purification is determining which seeds most effectively clean water. The effectiveness of the purification may depend on the size, maturity, growing season, color, or location of origin of the seeds. Isolating and quantifying MOCP can serve as a metric to differentiate seeds of varying water clarifying ability. Additionally, a method to purify MOCP is often a precursor to further study of this protein. In this work, young green seeds and mature brown seeds from Chiang Mai, India were found to contain 0.651% ± 0.056% and 1.21% ± 0.18% MOCP respectively. Additionally, brown seeds from Arcahaie, Haiti were composed of 0.456% ± 0.064% MOCP.

A second challenge with the f-sand column is the design and scale-up of a column for communities around the world. In highly controlled laboratory conditions, columns can be tested with a certain sand size and known water quality. However, it is crucial to see how these laboratory results apply to real conditions seen in developing countries. In order to address this

concern, this work aims to create a mathematical model representing the f-sand system to bridge the gap between laboratory and real world conditions. To accomplish this, classic environmental filtration models for particle removal were examined and applied to the f-sand system. Further, the electrostatic interactions specific to the f-sand column were studied to determine if they need to be incorporated into this model. The goal is for an end-user to be able to specify inputs such as column size, sand grain size, etc. and use the model to predict how much water the f-sand column will clean.

TABLE OF CONTENTS

LIST OF FIGURES v

LIST OF TABLES vi

ACKNOWLEDGEMENTS vii

Chapter 1 Introduction 1

Research Questions 2

Chapter 2 Background and Hypothesis 5

Previous Research on MOCP 5
Previous Research on Modeling 6
RT Model 10

Chapter 3 Materials and Methods 13

Preparation of Moringa Seeds 13
Solubilization of Protein 13
Cationic Protein Purification 14
Quantification of MOCP and Total Protein 16

Chapter 4 Modeling 19

Applying the RT Model to the F-sand System 19
Example Calculation with the RT Model 20
Electrostatic Forces and the Parallel Plate Model 26

Chapter 5 Results and Discussion 33

Results of Quantification 33
Results of Modeling 35

Chapter 6 Conclusions and Future Work 39

Protein Quantification Conclusions and Future Work 39
Conclusions on the F-Sand Modeling 40
Modeling Future Work 41

Appendix A Moringa Protein Purification and Quantification Protocol 43

Preparation of Moringa seeds....43
Quantification of total protein....43
Analyze data....44
Purification of MOCP....44
Quantification of Cationic Protein....45
Data Analysis of Quantification Results....46

Appendix B Example Standards Data and Graph....47

Appendix C Results of Chiang Mai Brown Seeds Quantification Experiment....49

References....51

LIST OF FIGURES

Figure 1: A Cationic Spin Column (Hoefer).....14

Figure 2: Comparing Experimental and Theoretical η.....24

Figure 3: Comparing F-sand and Control α.....25

Figure 4: Schematic of Parallel Plate System.....27

Figure 5: Comparison of Gravitational, Electrostatics, and Van der Waals Péclet Numbers..31

Figure 6: MOCP Quantification Results.....34

Figure 7: Total Protein Quantification Results.....34

Figure 8: Particle Radius, a vs. Fraction Increase in Collector Radius, h^*/a_c.....37

Figure 9: Comparison of Theoretical and Experimental Data with Modified Porosity.....38

Figure 10: Sample Standards Graph.....47

LIST OF TABLES

Table 1: Clean Bed Filtration Notation.....7

Table 2: Input Parameters for the F-sand Column.....19

Table 3: Input Parameters for the F-sand Column.....40

Table 4: Example Standards Data.....47

Table 5: Comparison of Standards Data.....48

Table 6: MOCP Quantification of Brown Chiang Mai Seeds.....49

Table 7: Total Protein Quantification of Brown Chiang Mai Seeds.....50

ACKNOWLEDGEMENTS

I would like offer thanks and admiration to my thesis advisor Dr. Stephanie Velegol for her invaluable mentorship. Your expertise and attention have made me a better engineer and person, and for that I am sincerely grateful.

Thank you to Dr. Darrell Velegol, for sharing his lab space and his intellect with modeling. Your unfailing patience and sage advice have made my undergraduate career a wonderful learning experience.

I would also like to thank my fellow undergraduate researchers, Kevin Shebek for his previous work in developing the purification and quantification procedure, Adam Uliana for providing experimental data and modeling support, Jenna Thomas for assistance through this writing process and finally, Emma Clement for many research efforts along the way. The future looks very bright for each of you and I wish you the best of luck.

Finally, I'd like to thank my honors advisor Dr. Eric Donnell and the Department of Civil and Environmental Engineering for all of their support.

Chapter 1

Introduction

The *Moringa oliefera* (Moringa) tree is indigenous to equatorial regions around the world. Many of these equatorial regions are poverty stricken and face severe water crises, so using Moringa seeds to purify water is an ideal solution that is sustainable, simple, and inexpensive. These seeds can clarify water due to the *Moringa oliefera* cationic protein (MOCP), which is a natural flocculent and antimicrobial agent. This antimicrobial activity stems from the structure of MOCP. MOCP consists of amino acids with primarily positively charge groups, but also some nonpolar functional groups. This structure allows the protein to interact and selectively kill microbes in water. Then through electrostatic interactions, MOCP causes microbes, dirt and other particles to stick to its surface, effectively removing them from water (Shebeck 2015).

However, directly placing Moringa seeds into contaminated water is only a temporary solution. While the MOCP cleans the water initially, the organic matter in Moringa seeds acts as a food source to microorganisms, promoting pathogen re-growth. In addition, this batch method only removes 90 – 99% of the microbes. This low removal is due to transport limitations. However, using functionalized sand (f-sand) addresses both of these challenges. F-sand is created when positively charged MOCP is adsorbed onto negatively charged sand particles, resulting in a net positive charge (Jerri 2012). The rest of the organic seed matter is then rinsed away, leaving f-sand that is capable of removing and killing microbes. Further, by packing the f-sand in a column, the microbes or other contaminants have a greater chance of sticking to the f-

sand and greater removal is possible. Therefore, it is more effective to adsorb this protein onto a sand column, and use the f-sand filter column to purify water. Prior research has shown that f-sand successfully reduces turbidity and kills certain microbes while avoiding the introduction of organic matter into the water. Specifically, this f-sand filter is capable of removing up to 99.999% of contaminants. These results are promising, but there are still several questions that need to be answered before the f-sand filter can be a solution to the water problem in developing countries.

Research Questions

Research Question #1: What percentage of Moringa seed is total protein and what percentage is MOCP?

In order to understand the purification ability of an f-sand column, further study of the clarifying agent MOCP is necessary. Moringa seeds come in various forms—young green seeds vs. mature brown seeds, seeds from Haiti vs. seeds from India, and seeds collected in the dry season vs. seeds collected in the wet season- and it is not known whether these differences affect the relative purification ability of the seeds. Quantifying the amount of MOCP in different varieties of seed gives a way to compare and predict the purification effectiveness of seed types. Although the total amount of protein in Moringa seeds has been studied (Ndabigengesere 1995), the MOCP concentration in Moringa seeds was undetermined prior to this research.

To quantify this protein, MOCP was separated from other proteins in Moringa seeds through a batch process. MOCP's defining feature, its strong cationic charge, can be used to

facilitate this separation via an ion exchange column. By repeating this batch process separation, enough MOCP can be concentrated for quantification of the protein. The protein concentration can then be measured using a colorimetric protein assay.

In the process of purifying MOCP, the total protein concentration in Moringa seeds is readily obtained. Total protein is easily purified through dissolution of the seeds followed by size separations. The percentage of total protein in Moringa can then be compared to estimates from other research.

Research Questions #2: How do we create a model to guide other users in creating an f-sand column? Do the electrostatic effects of Moringa seeds need to be included into this model?

A second goal of this research is to create a model that would allow users all over the world to create their own f-sand columns. Current testing in the laboratory has focused on using model microbe particles called sPSL or a more recently, a single species of bacteria. However, the conditions that the f-sand filter will experience in developing countries will contain a wide variety of microbes, dirt particles, and viral strains. A model needs to be created that can predict the purifying ability of f-sand in these highly controlled laboratory conditions and also adapt to the more variable conditions in developing countries.

The end goal of this model is for users to simply specify information about the features of the sand and column, and the model would predict how the f-sand column would attract and capture contaminant particles through mass transport. One challenge with predicting mass transport in the f-sand column is the electrostatic effect of MOCP. Since MOCP is positively

charged, the electrostatic force might affect the mass transfer of the system. This positive charge might not only affect how well contaminants stick once they reach f-sand particles, but could also affect the likelihood that the contaminants contact the f-sand particles. Clearly, further exploration of the electrostatic effect in contaminant particle capture is necessary.

Chapter 2

Background and Hypothesis

Previous Research on MOCP

Because of the growing interest in Moringa for water purification, significant study has been conducted on MOCP. MOCP is a dimeric protein with a molecular weight of 13 kDa, with each monomer unit weighing 6.5 kDa (Ndabigengesere 1995). This protein contains high levels of the following amino acids: glutamine, a polar amino acid; argentine, an amino acid with a positively charged side chain, and proline, an uncharged amino acid (Gassenschmidt 1994). It is the combination of hydrophilic groups surrounding hydrophobic groups arranged in a helix-loop-helix motif that allows MOCP to interact and selectively kill microbes in water (Suarez 2005), (Shebeck 2015). Additionally, this composition creates an overall positive surface charge measuring at 2 mC/m^2 and a zeta potential of 70 ± 15 mV in a solution of 0.5 mM KCl (Bechtel 2015). MOCP's relatively low molecular weight, combined with a high charge density is what gives MOCP its flocculating ability (Gassenschmidt 1994).

Measuring the concentration of MOCP in Moringa seeds is important because it gives us a metric to compare the flocculating ability of different types of Moringa seeds or to compare to other flocculating agents. However, there have been no documented attempts to quantify the cationic protein content in Moringa seeds, and this research hopes to fill this knowledge gap. It is also of interest to measure the total protein content to see how much of the total protein in the seed is composed of MOCP. Other research has approximated the total protein content of these seeds by measuring the nitrogen levels in Moringa seed. Since nitrogen in seeds is primarily

found in proteins only, the nitrogen levels correlate to the amount of protein present. For shelled seeds, the total protein content is estimated to be about 35% of the seed mass (Ndabigengesere 1995). This research hopes to produce a more direct measurement of total protein.

Previous Research on Modeling

There are many models for water filtration that can be used to help form a model for f-sand particle removal. Each of the models we examined is classified as a "clean bed filtration model." Clean bed filtration theory assumes that the collector (an f-sand particle) is an infinite sink for contaminant particles (sPSL, *E. coli*., etc.) flowing past (Yao 1971). Clearly, this assumption holds well during the start-up of filtration, and begins to fail as particles build up on the collector surface. For this work, we will focus solely on the start-up of water purification, when clean-bed assumption is valid. Further information can be found on clean-bed filtration in Environmental Transport Processes by Bruce Logan (Logan 1999), (Logan 2002). The clean-bed filtration derivation that follows has been adapted from this text.

To assist the reader, a table of variables is given below. All variables are given in SI base units form for ease of computation. Additionally, these variables will be re-introduced through the text.

Table 1: Clean Bed Filtration Notation

Table of Notation

A	Hamaker constant for van der Waals interactions, ranges from 10^{-19}-10^{-21} (J)
A_c	Cross-sectional Area (m^2)
A_v	Surface area per volume (m^2/m^3)
b_H	Constant that accounts for concentric flow around collectors in a packed bed; porosity dependant
d_p	Diameter of a contaminant particle (m)
d_c	Diameter of a collector (m)
g	Standard gravitational acceleration, 9.8 m/s^2
k_B	Boltzmann constant, $1.3806x10^{-23}$ kg $m^2/(s \times m)$
L	Length of the column (m)
Lo	Dimensionless constant that accounts for van der Waals interactions
N	Moles of particles that elute from the column (moles)
N_0	Moles of particles that enter the column (moles)
T	Temperature (K)
t	Time (s)
u	Pore Velocity $u=U/\Theta$ (m/s)
U	Darcy, approach, or superficial velocity; velocity of fluid as it enters the column (m/s)
Q	Flow rate of fluid through the porous column (m^3/s)
z	vertical coordinate from the top (z=0) to bottom (z=L) of the column (m)

Greek Letters

α	Sticking coefficient, ratio of the rate particles stick to the collector to rate particles that strike the collector
γ	Function of porosity; term used to simplify calculation of b_H
η	Single collector collision efficiency, ratio of the rate particles strike collector to rate particles flow towards collector
η_D	Collector efficiency due to diffusion
η_I	Collector efficiency due to interception
η_S	Collector efficiency due to gravitational sedimentation
ρ_f	Density of the fluid, kg/m^3
ρ_p	Density of a particle, kg/m^3
μ	Dynamic fluid viscosity, kg/(s x m)

The clean –bed transport equation can be derived by starting with a basic mass balance over a control volume (Logan 1999):

$$accumulation = in - out \quad \textbf{Eq 1}$$

The accumulation term of the contaminant particles on the collectors within the control volume can then be defined:

$$accumulation = \frac{3\alpha\eta(1-\theta)NA_v U\Delta z\Delta t}{2d_c} \quad \textbf{Eq 2}$$

where d_c is the collector diameter, N is the number of moles, A_v is the surface area divided by volume, and U is the superficial velocity. The accumulation is taken over a thickness Δz and over time Δt. η is the fraction of particles that reach a collector surface to the total number of particles flowing past the surface. Essentially, η is a summation of the different transport methods that bring a particle in contact with a collector, which is a function of temperature (T), particle diameter (d_p), collector diameter (d_c), superficial fluid flow rate (U), density of particle (ρ_p), column porosity (Θ), and Hamaker constant (A). η is often referred to as the collector efficiency. α is the fraction of particles that stick to the collector after they collide with the collector, and is often referred to as the stickiness fraction.

The in and out terms from Equation 1 are comprised from two transport terms, advection and dispersion. With advection, contaminant particles enter and exit in a time period Δt due to fluid flow velocity, U.

$$advection = N_z AU\Delta t - N_{z+\Delta z} AU\Delta t \quad \textbf{Eq 3}$$

Dispersion occurs via molecular diffusion of contaminant particles coming in and out of the control volume. The dispersion component is composed of the molar flux multiplied by cross-sectional area, A_c. The flux term follows Fick's first law, with diffusion coefficient D_L:

$$dispersion = -\left(D_L A_c \theta \Delta t \frac{dN_z}{dz} - D_L A_c \theta \Delta t \frac{dN_{z+\Delta z}}{dz}\right) \quad \textbf{Eq 4}$$

Combining Equations 2-4, and rearranging term gives:

$$-UA_c \frac{(N_{z+\Delta z} - N_z)}{\Delta z} + \frac{D_L A_c \theta \left(\frac{\partial N_{z+\Delta z}}{\partial z} - \frac{\partial N_z}{\partial z}\right)}{\Delta z} = \theta A_c \frac{\Delta N}{\Delta t} + \frac{3}{2d_c}(1-\theta)\alpha\eta A_c N U \quad \textbf{Eq5}$$

From Equation 5, the cross-sectional area terms can be canceled and the limit as Δz and Δt goes to zero can be taken. Additionally, the superficial velocity U equals the pore velocity, u, times the porosity, Θ.

$$\frac{\partial N}{\partial t} + u\frac{\partial N}{\partial z} - D_L \frac{\partial^2 N}{\partial z^2} + \frac{3}{2d_c}(1-\theta)\alpha\eta u N = 0 \quad \textbf{Eq6}$$

Recognizing that the adjective transport will dominate over dispersive transport of contaminant particles entering and exiting the control particles, the dispersion term can be neglected. Additionally, a steady state assumption eliminates the time derivative, resulting in Equation 7.

$$\frac{\partial N}{\partial z} = -\frac{3}{2d_c}(1-\theta)\alpha\eta N \quad \textbf{Eq7}$$

Integrating over the entire column length, results in an equation for particle removal.

$$\frac{N}{N_0} = \exp\left(\frac{3}{2d_c}(1-\theta)\alpha\eta L\right) \quad \textbf{Eq 8}$$

Equation 8 is a classic equation that is the basis for all clean-bed models. Clean-bed models differ by changing the assumptions in the calculation of the η, the collector efficiency.

RT Model

The model we selected to use to model the f-sand column is called the Rajagopalan and Tien (RT) model (Rajagopalan 1976), (Logan 1999). The primary assumption for the RT model is that the fluid flow occurs concentrically around the collector. This creates a fluid layer that is evenly dispersed around each collector particle. To account for this fluid layer, a constant dependent on porosity, b_H, is created:

$$b_H = \left(\frac{2(1-\gamma^5)}{2-3\gamma+3\gamma^5-2\gamma^6}\right) \quad \textbf{Eq 9}$$

$$\gamma = (1-\theta)^{1/3}$$

Additionally, the RT model accounts for attraction between particles and collectors due to London-van der Waals forces and from the lubrication effect with the inclusion of Lo.

$$Lo = \frac{4A}{9\pi\mu d_p^2 U} \quad \textbf{Eq 10}$$

where A is the Hamaker constant. Typical Hamaker constants range from 10^{-21}-10^{-19}.
The Lo and b_H factors are included in the collector efficiency terms.

η is comprised of mass transport processes, namely diffusion, interception, and gravitational sedimentation. Diffusion based collisions (η_D) occur when a particle collides with a collector due to its Brownian motion. Diffusion has a much greater influence on smaller particles than larger ones. An equation can be obtained for η_D by using empirically obtained mass transport correlations. For these correlations, it assumed that the dimensionless Péclet

number, the ratio of advective transport to diffusive transport, is high because of forced convection and that the Reynolds number is low.

$$\eta_D = 4.04 b_H^{1/3} Pe^{-2/3} = 0.9 b_H^{1/3} \left(\frac{k_B T}{\mu d_c d_p U} \right)^{2/3} \quad \textbf{Eq 11}$$

Particles collide via interception (η_I) when the fluid flow carries the particles on a streamline that traverses a collector. Oppositely of diffusion, interception dominates for larger particles. Like in the correlation for diffusive transport, interception includes a b_H term to account for the fluid layer around the particles.

$$\eta_I = b_H Lo^{1/8} \left(\frac{d_p}{d_c} \right)^2 \quad \textbf{Eq 12}$$

Lastly, particle collisions due to gravitational sedimentation arise when the settling velocity of the particle overcomes the streamline motion of the fluid. The (η_S) is therefore a ratio of the settling velocity from Stokes law to the streamline velocity. Gravitation sedimentation generally has the smallest contribution to the transport of particles; however like interception, it increases with increasing particle size.

$$\eta_S = 0.00338 b_H \left(\frac{g \Delta \rho}{18 \mu U} (d_p)^2 \right)^{1.2} \left(\frac{d_p}{d_c} \right)^{-0.4} \quad \textbf{Eq 13}$$

Summing Equations 11, 12, and 13, results in a total η.

$$\eta_{Total} = \eta_D + \eta_I + \eta_S \quad \textbf{Eq 14}$$

With values of η and α, Equation 8 can be used to predict the percentage removal of contaminant particles. This is important for modeling an f-sand filter. The RT model shown here is a good starting point for this modeling, and Chapter 4 shows the results of RT for the f-sand system. However, the RT model does not include the electrostatic interactions of f-sand, so further investigation is needed to determine if electrostatics forces need to be incorporated into the f-sand model.

Chapter 3

Materials and Methods

To determine the percentage of MOCP, a purification and quantification procedure was developed. The procedure can be divided into 4 parts: preparation of the Moringa seeds, purification of the total protein, purification of the cationic protein, and quantification of total and cationic protein. Breaks in time can be taken between each of these 4 parts, however when a part is started, we recommend that it is completed all the way through without stopping. The following outlines the methodology and theory behind this protocol. Appendix A outlines this same procedure in a more stepwise fashion.

Preparation of Moringa Seeds

Estimated time: 20-30 minutes

First, ten seeds were chosen at random from a bag containing seeds collected at the same time and location. The seeds were shelled and then grinded in a coffee grinder until they became a fine powder. A motor and pestle or any other crushing device is also sufficient. The grinded seeds labeled with the date crushed and seed type were stored in a covered container at room temperature until needed.

Solubilization of Protein

Estimated Time: 10-15 min of lab work, 1 hour on the stir plate

Our next step was to solubilize the protein from the powdered Moringa seeds. 0.1 g of seed was added to 10 mL of DI water, and the solution was subsequently mixed for one hour on a stir plate. This time is currently being investigated by other students and may be able to be shortened. The bulk seed solution was then filtered twice: first with 5 μm filter paper, followed by a 0.2 μm syringe filter (VWR International, Cat. 28145-501). The bulk seed solution was saved for later purification of the cationic protein (MOCP) and for the quantification of the total protein. There will be enough bulk protein solution for both. This solution contains a high amount of total organic carbon, so it should be refrigerated or preferably frozen to prevent microbe growth during storage.

Cationic Protein Purification

Estimated Time: 6-7 hours

If the solubilized protein solution was frozen, allow to completely thaw before proceeding. Using this solution, we sought to isolate MOCP using a weakly cationic spin column (Hoefer, Cat No. SP-744207).

Figure 1: A Cationic Spin Column (Hoefer)

Since MOCP is a strongly charged cationic protein, a weakly cationic spin column absorbs MOCP almost exclusively in the resin, while limiting the absorption of less positively charged proteins. The spin column was centrifuged frequently during this procedure to elute undesired proteins and solvent. All centrifuge cycles were performed at 2000g for 2 minutes unless otherwise specified. Shorter centrifugation times of 1 minute were tried, but that led to less MOCP protein. Longer centrifuge times of 5 and 7 minutes were also attempted, but they yielded similar amount of protein as 2 minute centrifugation.

The spin column was first hydrated with DI water for 10 minutes, and centrifuged to remove excess water. 200 µl of the bulk seed solution was added to the spin column and centrifuged. The eluent was loaded back into the spin column and centrifuged again to ensure maximum absorption of MOCP to the resin. The eluent was then discarded, and another 200 µl was added to the spin column, following the same centrifugation and reloading procedure as the first. Then, 200 µl of DI water was added to the spin column and centrifuged. This washing removes any protein that remained weakly absorbed to the resin, and is completed twice. To concentrate the MOCP enough for quantification, this process, starting with the first addition of 200 µl of bulk solution, is repeated until 3 mL of bulk solution has been loaded through the spin column. This means the 200 µl of bulk solution has been loaded and reloaded 15 times.

The column was then loaded with 200 µL of 0.2 M NaCl and centrifuged in order to remove any weakly bound proteins while keeping the MOCP bound to the resin. To elute MOCP, 200 µl of 0.6M NaCl was repeatedly loaded into the column and centrifuged until 3 ml of eluent was obtained and saved in Eppendorf tubes. MOCP elutes at salt concentrations of

0.6M-1M, so only the second salt solution significantly removes MOCP (Ndabigengesere 1995). The resulting solution underwent refrigerated dialysis to remove excess salt and to transfer the MOCP to a phosphate buffered saline solution (137 mM NaCl, 2.7 mM KCl, 10 mM Na_3PO_3, 1.8 mM KH_2PO_4 , pH = 7) which keeps the MOCP from fouling or precipitating. Dialysis was completed in 3.5K MWCO cassettes (Thermo Scientific Slide-A-Lyzer), but can also be completed using dialysis tubing. This dialysis is only necessary if further study of the MOCP protein is desired; otherwise it can be omitted.

Quantification of MOCP and Total Protein

Estimated time: 2 hours for quantification, 1 hour to make standards

The concentration of the total protein and cationic protein was quantified using BSA protein assay (BSA Standard, Pierce protein Biology Products, Cat No. 23225). The unknown amount of protein in Moringa seed must be compared to standards of known protein composition. These standards are produced from a serum containing 2 mg/mL of protein(BSA Standards Ampules, Cat No. 23209). Using a combination of this serum and DI water, nine different compositions of standard ranging from 0-2000 mg/L are created. When the standards are made, they can typically be used for approximately ten quantifications, before running out, assuming standards are tested in triplicate.

Both standards and unknown Moringa samples were quantified in triplicate, allowing the 3 results for each sample to be averaged. Working reagent (WR) that will react with proteins to

create a color change can be made by following the procedure dictated in the BSA kit instructions. To find the volume of WR needed, the following formula was used:

$$3(\#\ of\ samples\ +\ 9\ standards +\ 5) \times\ 200\ \mu l\ of\ WR = Volume\ of\ WR\ in\ \mu l \quad \textbf{Eq 15}$$

The "3" in the beginning of Equation 15 accounts for the number of replications of the same protein sample, which is 3 since each standard and Moringa sample is quantified in triplicate. The "5" added to the number of standards and samples ensures an extra amount of Working Reagent is produced to preventing running out.

Because of the reactive nature of the WR, it will react with itself if stored for longer than a day. Thus, the BSA protein assay kit contains two storable solutions, a large bottle of colorless WR A and a smaller bottle of blue WR B, that must be mixed together to produce the WR used for quantification. WR A and WR B are mixed in a ratio of 50:1. After using Equation 15 to find out the total amount of Working Reagent, the amount of components A and B can be calculated by:

$$Volume\ of\ WR\ A = \frac{50(Volume\ of\ total\ WR)}{51} \quad \textbf{Eq 16}$$

$$Volume\ of\ WR\ B = \frac{(Volume\ of\ total\ WR)}{51} \quad \textbf{Eq 17}$$

Mixing WR A and WR B in the correct amounts produces a green WR.

10 µl of standard or Moringa sample and 200 µl of BSA working reagent were added to a labeled Eppendorf tube. Each Eppendorf tube was placed in an Eppendorf tube rack, and the rack was gently shaken to mix the working reagent and protein sample together. The rack was

then placed into a heat bath at 37°C to allow the color-changing reaction to take place. After 30 minutes, the rack was taken out, and the samples and standards were pipette into a 96 well microplate. Wells containing a high amount of protein should be a dark purple color while wells containing little protein should be a light green. The absorbance of each sample and standard was then measured using a microplate reader (Molecular Devices, Spectra Max Plus 384) and Soft Max Pro plate reader software set at a wavelength of 562nm.

From there, a quantification curve can be constructed from the standards to determine the protein concentration of the Moringa samples (Appendix B). The concentration can be normalized over the starting weight of the Moringa seeds to obtain the percentage of MOCP in the seeds.

Chapter 4

Modeling

Applying the RT Model to the F-sand System

The RT model for the f-sand system is a function of 9 independent parameters: temperature, particle diameter, collector diameter, fluid flow rate, column diameter, density of particle, column porosity, Hamaker constant and column length. Shown in Table 2 is an example f-sand system with these parameters specified, using silica sand collectors and sPSL as the model particle. Along with these parameters, a standard deviation was given based on the range of observed values in typical laboratory conditions. If this range was not known, the standard deviation was estimated by taking 10% of the original value.

Table 2: Input Parameters for the F-sand Column

Input Parameters	**Example Value**	**Units**	**Typical Ranges**
T	298 ± 10	K	273-310K
d_p, particle diameter	$2.90 \times 10^{-6} \pm 8.99 \times 10^{-8}$	m	10^{-8}-10^{-5}m
d_c, collector diameter	$2.10 \times 10^{-4} \pm 2 \times 10^{-5}$	m	10^{-4}-10^{-3}m
Q, flow rate (vA)	$1.05 \times 10^{-8} \pm 1.05 \times 10^{-9}$	m^3/s	----------*
D, Diameter of the column	0.01 ± 0.001	m	----------*
ρ_p, Density of particle	1050 ± 2.89	kg/m^3	----------
Θ, porosity	0.36 ± 0.036		0.25-0.70
A, Hamaker constant	$1.4 \times 10^{-20} \pm 1.41 \times 10^{-21}$	J	10^{-21}-10^{-19}J
L, Length	0.1 ± 0.01	m	----------*

*****Parameters depend on the scale of the column

Because of the electrostatic forces in f-sand, it can be assumed that α=1, meaning that every particle that hits a collector will stick. Additionally, the collectors ranged from 210 μm- 290 μm, but a single particle diameter size of 230μm was used in this example calculation. Approximately 10% or less of the particles had a diameter of 230 μm or less (D10). The D10 was chosen over the average diameter (D50) because smaller particles are responsible for greater contaminant removal (Paramonova 2006). Also, error in measuring the 9 parameters in Table 2 tends to skew the data upward due to the nonlinearity of the RT model, so using a lower estimate for collector diameter is preferred.

Example Calculation with the RT Model

With this assumption about α and the 9 parameters specified, the filtration equation can be solved for this system. First, the Darcy (approach) velocity was calculated from an experimentally acquired flow rate, Q. The flow rate was obtained by measuring the time it took to elute 10 mL from the column. Dividing by the surface area of the column converts this flow rate to a pore velocity. Pore velocity will always be greater than the approach velocity due to the column's pores, which reduce surface area available for flow. Thus, to obtain the Darcy velocity, the pore velocity must be multiplied by porosity.

$$U = \frac{Q\theta}{\pi\left(\frac{d_{column}}{2}\right)^2} = \frac{1.05 \times 10^{-8}\frac{m^3}{s} \times 0.36}{\pi\left(\frac{0.1m}{2}\right)^2} = 4.81 \times 10^{-5}\frac{m}{s} \quad \textbf{Eq 18}$$

Next, the effects of van der Waals forces, lubrication, and concentric fluid layer were accounted for with the Lo and b_H constants. For sPSL, the Hamaker constant was approximated as 1.4 x 10^{-20} J (Velegol, 2012).

$$\gamma = (1-\theta)^{1/3} = (1-0.36)^{1/3} = 0.862 \quad \textbf{Eq 19}$$

$$b_H = \left(\frac{2(1-\gamma^5)}{2-3\gamma+3\gamma^5-2\gamma^6}\right) = \left(\frac{2(1-0.862^5)}{2-3\times 0.862+3\times 0.862^5-2\times 0.862^6}\right)$$

$$= 49.096 \quad \textbf{Eq 20}$$

$$Lo = \frac{4A}{9\pi\mu d_p^2 U} = \frac{4\times 1.4\times 10^{-20}\,\frac{kg\times m^2}{s^2}}{9\pi\times 0.000891\,\frac{kg}{s\times m}\times (2.9\times 10^{-6}m)^2\times 4.81*10^{-5}\,\frac{m}{s}}$$

$$= 0.00549 \quad \textbf{Eq 21}$$

Then, the collector efficiency for diffusion, interception, and gradational sedimentation were calculated, and summed to find the total collector efficiency η.

Diffusion Collector Efficiency:

$$\eta_D = 0.9 b_H^{1/3} \left(\frac{k_B T}{\mu d_c d_p U} \right)^{2/3}$$

$$= 0.9 * 49.096^{1/3} \left(\frac{1.38 * 10^{-23} \frac{kg \times cm^2}{s^2 \times K} \times 298K}{\left(0.000891 \frac{kg}{s * cm}\right) \times (2.9 * 10^{-6} m) \times (2.3 \times 10^{-6} m) \times (4.81 \times 10^{-5} \frac{m}{s})} \right)^{2/3}$$

$$= 0.0090 \quad \textbf{Eq 22}$$

Interception Collector Efficiency:

$$\eta_I = b_H Lo^{1/8} \left(\frac{d_p}{d_c} \right)^2 = 49.096 \times 0.00549^{1/8} \left(\frac{2.9 \times 10^{-6} m}{2.3 \times 10^{-6} m} \right)^2 = 0.0070 \quad \textbf{Eq 23}$$

Gravitational Collector Efficiency:

$$\eta_S = 0.00338 b_H \left(\frac{g \Delta \rho}{18 \mu U} (d_p)^2 \right)^{1.2} \left(\frac{d_p}{d_c} \right)^{-0.4}$$

$$= 0.00338 \times 4 \times \left(\frac{9.8 \frac{m}{s^2} \times (1050 - 997.13) \frac{kg}{m^3}}{18 * 0.000891 \frac{kg}{s * cm} * 4.81 * 10^{-5} \frac{m}{s}} \right)^{1.2} \left(\frac{2.9 * 10^{-6} m}{2.3 * 10^{-6} m} \right)^{-0.4}$$

$$= 0.0019 \quad \textbf{Eq 24}$$

Total Collector Efficiency:

$$\eta_{Total} = \eta_D + \eta_I + \eta_S = 0.0090 + 0.0080 + 0.0019 = 0.0180 \quad \textbf{Eq 25}$$

Clearly, diffusion and interception are the dominating transport processes contributing to collector efficiency for this system. However, η_s is still within the same order of magnitude as η_D and η_I, and therefore is not negligible.

By Equation 25, the theoretical total collector efficiency was found to be η=0.0180. Error bars can be calculated for this η value by using the parameters in Table 2 and the parameter's associated standard deviation. Since the error for each parameter represents not just one value, but a range, the amount of standard deviation added to the original value was determined by a random Gaussian number generator. These random numbers were generated in Excel using the function "NORMINV(RAND(), Mean, SD)" where RAND specifies a random probability in the Gaussian distribution, Mean is the original parameter value, and SD is the standard deviation of each parameters. The random Gaussian value for each parameter was calculated 100 times, and η was calculated for each iteration. Using the standard deviation of the 100 η trials, the 95% confidence interval can be determined for η. For the conditions in Table 2, the range of η values was calculated to be from 0.0190-0.0201. Note that the originally calculated η value falls below of this 95% confidence range. This is due to the nonlinearity of the formulas in the RT model; any addition of error tends to skew the data upward from its original value.

Additionally, η=0.0180 theoretical value can be compared to experimental data at the same conditions. Two experimental trials (f-sand 1 and f-sand 2) were conducted with approximately 10^7 particles/mL entering the column (Uliana 2014). The experimentally measured N/N_0 value and the assumption of α=1 can be used to calculate $\eta_{experimental.}$

$$\eta_{experimental} = \frac{-2d_c}{3(1-\theta)L\alpha\eta} \ln\left(\frac{N}{N_0}\right) \quad \textbf{Eq 26}$$

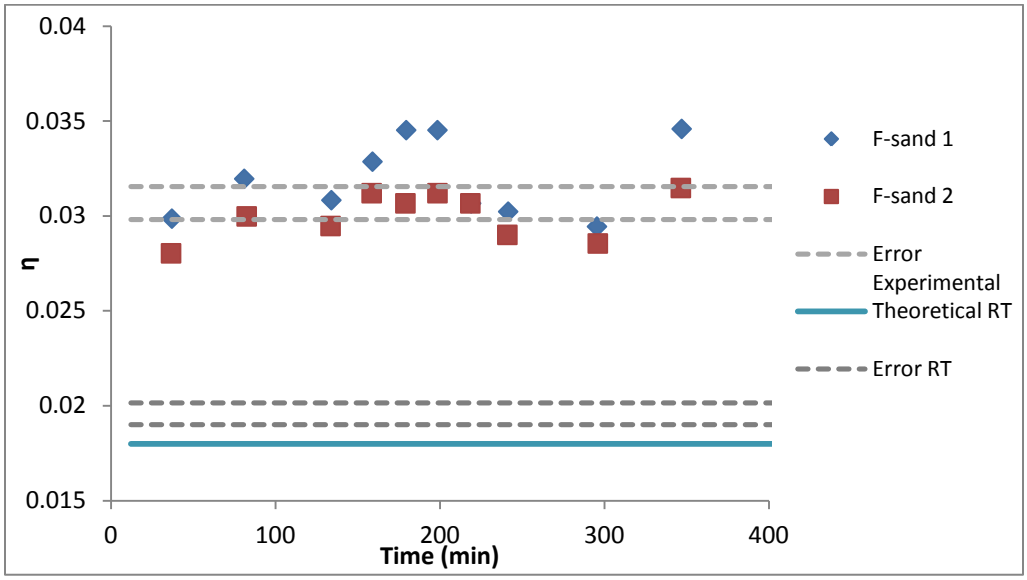

Figure 2: Comparing Experimental and Theoretical η

As seen in Figure 2, the predicted η value is consistently lower than the experimentally determined η, meaning that there are more particles removed than would be predicted with this model. This discrepancy between η values can be due to experimental error or a missing assumption from the model.

Alternatively, the experimental data and model predictions can also be compared by calculating an experimental α value instead of an experimental η. The theoretical value of η=0.0180 can be used for the collector efficiency, and the experimental data can be used to calculate α for the same two f-sand samples as in Figure 2 as well as a control sample that had bare sand without any Moringa protein.

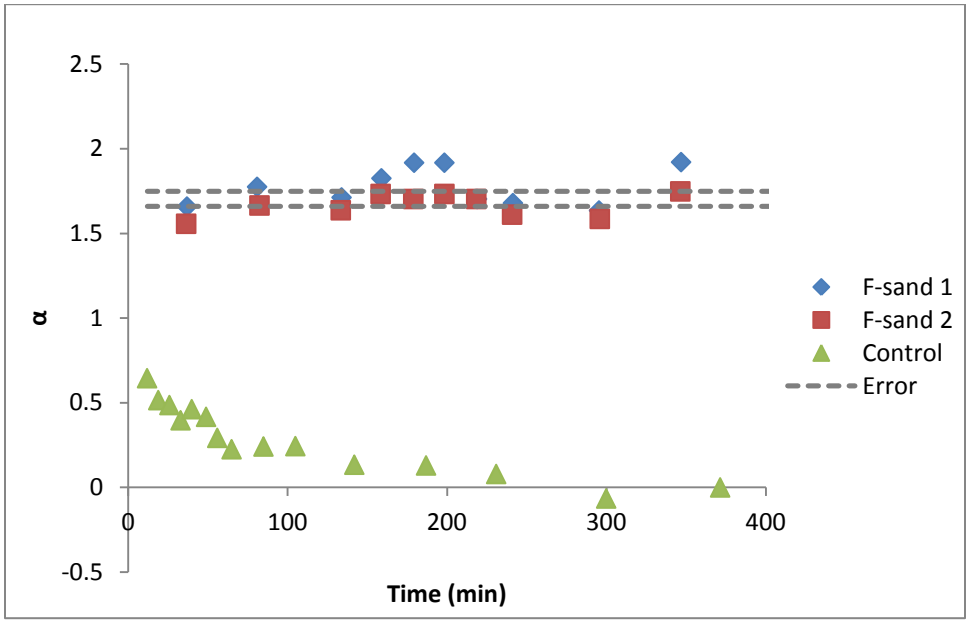

Figure 3: Comparing F-sand and Control α

The f-sand α was calculated to be α=1.705 ± 0.044 while the control exhibited too much variance to obtain a reasonable average for α within the 400 minute span. The control however always demonstrated an α value less than the theoretical maximum of 1. For the f-sand samples, the α value was consistently greater than 1, which has no physical meaning. Ideally, α should always be less than or equal to one because the total number of particles that collide with the collector should be greater than the total number of particles that stick to the collector. However in some instances, researchers used α values greater than 1 to account for non-idealities in their system (Paramonova 2006).

$\eta_{experimental}$ may be different than theoretical η and the experimental α may be greater than 1 for several different reasons. First, there may be an experimental error. This experiment will have to be completed several more times to ensure the results remain consistent. Another possibility is that the RT model does not account for when electrostatic forces affect the

likeliness of a particle to strike a collector. Depending on particle size, flow rate, and salt concentration, electrostatic forces may or may not have an effect in the collector efficiency.

Electrostatic Forces and the Parallel Plate Model

In the current RT model for the f-sand filter, electrostatic interactions are only incorporated in the α term, meaning electrostatics forces govern the "stickiness" of particle-collector interactions. Frequently in other research, an α term greater than one is used to account for electrostatic effects (Paramonova 2006) However, since α is a ratio of particles that collide with the collector to the total number of particles, an α greater than one has no physical interpretation.

There are two alternatives other than grouping the electrostatic effects with α. First, electrostatic interactions can be incorporated into the collector efficiency term η. A new η_E could be defined to account for the increase in collector efficiency due to the positive charge pulling particles into the collector surface. Another option for including electrostatic interactions is to change the porosity. In this view, electrostatic interactions are essentially creating a larger effective radius for collector particles, which would decrease the porosity value.

Before figuring out if electrostatic interactions are best incorporated in η or porosity, we first must determine how important these interactions are to attracting and capturing particles. To determine this, we can use a model parallel plate particle system, shown in Figure 4.

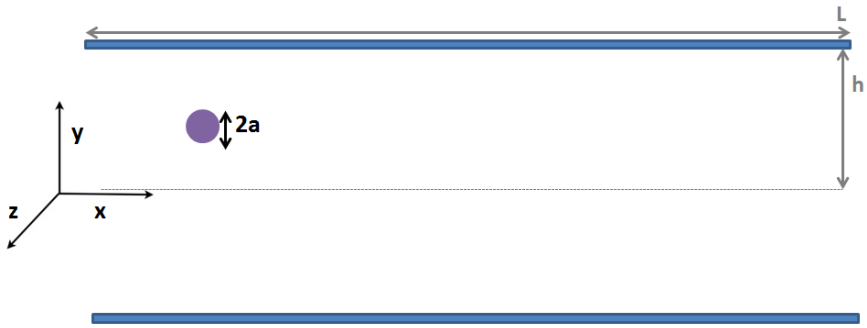

Figure 4: Schematic of Parallel Plate System

These parallel plates represent a simplified version of a collector rather than the more mathematically complex spherical collector. The parallel plate system is very well defined in mathematics and engineering, making this an ideal model system. Figure 4 shows this parallel plate system, with plate of length L (x-direction), separated by a distance of length 2h (y-direction). The width of the plates in the z-direction can assumed to be infinite.

A particle begins at x=0 and a random y-coordinate. Then, the particle is sent through the parallel plates by the effects of flow, external forces, and random Brownian motion. Eventually, the particle may hit the plate, and "stick", meaning it is captured by the collector. We will assume that α=1, meaning that all particles that collide with the plate stick.

To assess the importance of electrostatic forces in this model, the average perpendicular Péclet (Pe) number can be calculated for different external force values, and compared to each other. The Péclet number is defined as follows:

$$Pe = \frac{advective\ transport}{diffusive\ transport} = \frac{UL}{D} \quad \textbf{Eq 27}$$

where D is the diffusion coefficient, U is the y-direction fluid velocity, and L is the characteristic length. Therefore, high Péclet numbers signify that advection, the bulk motion of the fluid, dominates. In contrast, a low Péclet number indicates that diffusion, random molecular movement is the dominant transport method.

The distance h can be used as the characteristic length and to non-dimensionalize the Péclet number as follows.

$$Pe = \frac{\int_0^h \frac{Uh}{D} dh}{h} \quad \textbf{Eq 28}$$

With distance h specified by the length of the plate, it remains that the diffusion coefficient and fluid velocity must be defined. The diffusion constant can be estimated by the Stokes-Einstein equation:

$$D = \frac{k_B T}{6\pi\eta a} \quad \textbf{Eq 29}$$

The fluid velocity in the y-direction as described by Stokes' law:

$$U = \frac{F}{6\pi\eta a} \quad \textbf{Eq 30}$$

In Equation 30, F is the summation of external forces that act on the particle. Substituting Equations 29 and 30 into 28 yields:

$$Pe = \frac{\int_0^h \frac{F}{kT} dy}{h} \quad \textbf{Eq 31}$$

Equation 31 can be non- dimensionalized by defining distance w=y/h as the dimensionless distance between the plate wall and the contaminant particle.

$$Pe = \frac{\int_0^h \frac{F}{kT} w\, h dw}{h} = \int_0^h \frac{F}{kT} w\, dw \quad \textbf{Eq 32}$$

With Equation 32, separate Péclet number can be calculated for each of the external forces that act on the particle, namely gravitational force (F_g), van der Waals force (F_{vdw}) and the electrostatic force (F_{es}). This separate integration can be done since the external forces sum linearly. This allows for the comparison of the relative magnitudes of the Gravitational, Electrostatic and Van der Waals Péclet number.

For the Gravitational Péclet number, the gravitational force can be defined by applying Stokes' law on the buoyancy of a spherical particle.

$$F_g = \frac{4}{3}\pi a^3 (\rho_p - \rho_f) g \quad \textbf{Eq 33}$$

Integrating this force over the dimensionless variable w yields the Gravitational Pe number. Using a distance of h=1, the bounds become from 0 to 1.

$$w = \frac{y}{h}$$

$$Pe_g = \frac{F_g h}{kT} \int_0^1 w\, dw = \frac{\frac{4}{3}\pi a^3 (\rho_p - \rho_f) g h}{kT} \left(\frac{1}{2} w^2\right) \begin{matrix} w = 1 \\ w = 0 \end{matrix}$$

$$Pe_g = \frac{\frac{2}{3}\pi a^3 (\rho_p - \rho_f) g h}{kT} \quad \textbf{Eq 34}$$

Electrostatic forces can be modeled using theory for electrostatic double layer (EDL) that describes the behavior of charged surfaces. The f-sand filter is governed by EDL interactions; the negatively charged sand and positively charged MOCP interact to form a compact double

layer, and microbes and the MOCP interact to form a more diffuse second layer. The distance over which the charge separation between the MOCP and microbes can occur is called the Debye length, κ^{-1}. The inverse Debye length is defined as:

$$\kappa = \sqrt{\frac{\varepsilon_r \varepsilon_0 RT}{2F^2 C_0}} \quad \textbf{Eq 35}$$

The force of an electronic double layer is then:

$$F_{es} = \pi\kappa\varepsilon a\zeta_p\zeta_c \mathrm{e}^{-\kappa(h-a+y)} \quad \textbf{Eq 36}$$

where ζ represents the zeta potential of the particle (ζ_p) and collector (ζ_c).

Like the Gravitational Péclet number, the force equation for EDL can be substituted in Equation 28 and integrated to solve the Electrostatics Péclet number.

$$Pe_{es} = \int_0^1 \frac{F_{es} hw}{kT}\, dw \quad \textbf{Eq 37}$$

$$Pe_{es} = \frac{\pi\varepsilon a\kappa\zeta_p\zeta_w h}{kT}\int_0^1 e^{-\kappa(h-a+w)} dw \quad \textbf{Eq 38}$$

$$Pe_{es} = \frac{\pi\varepsilon_0\varepsilon_r a\zeta_p\zeta_w \mathrm{e}^{(\mathrm{a}-2\mathrm{h})\kappa}\left(-1+\mathrm{e}^{\mathrm{h}\kappa}-\mathrm{h}\kappa\right)}{kTh\kappa} \quad \textbf{Eq 39}$$

Equation 39 can be further simplified by assuming that the -1-hκ term is negligible. Since the inverse Debye length is on the order of 10^8, $\mathrm{e}^{\mathrm{h}\kappa}$ will grow much larger than -1-hκ.

$$Pe_{es} = \frac{\pi\varepsilon_0\varepsilon_r a\zeta_p\zeta_w\left(\mathrm{e}^{-\kappa(\mathrm{h}-\mathrm{a})}\right)}{kTh\kappa} \quad \textbf{Eq 40}$$

Lastly, the van der Waals Péclet number can be calculated. Van der Waals force is the attractive force between molecules with induced dipoles.

$$F_{vdw} = \frac{-Aa}{6(h-a+y)^2} \quad \textbf{Eq 41}$$

$$Pe_{vdw} = \frac{h}{kT}\int_0^1 F_{vdw} w\, dw = \frac{-Aa}{6kT}\int_0^1 \frac{w}{\left(1 - \frac{a}{h} + w\right)^2} dw \quad \textbf{Eq 42}$$

$$Pe_{vdw} = \frac{-Aa}{6kT}\left[\frac{h - (a - 2h) * \left(\ln\left(1 - \frac{a}{h}\right) - \ln\left(2 - \frac{a}{h}\right)\right)}{a - 2h}\right] \quad \textbf{Eq 43}$$

Then, the f-sand parameters from Table 2 are put into the Péclet equations (34, 39, 43). To see where the electrostatic interactions are most relevant, the Electrostatics Péclet number can be compared to the Gravitational and Van der Waals Péclet numbers at varying h values, i.e. varying distances between the contaminant particle and collector. When choosing h values, h can never be less than the radius of the particle (a=1.45 x 10^{-6} m).

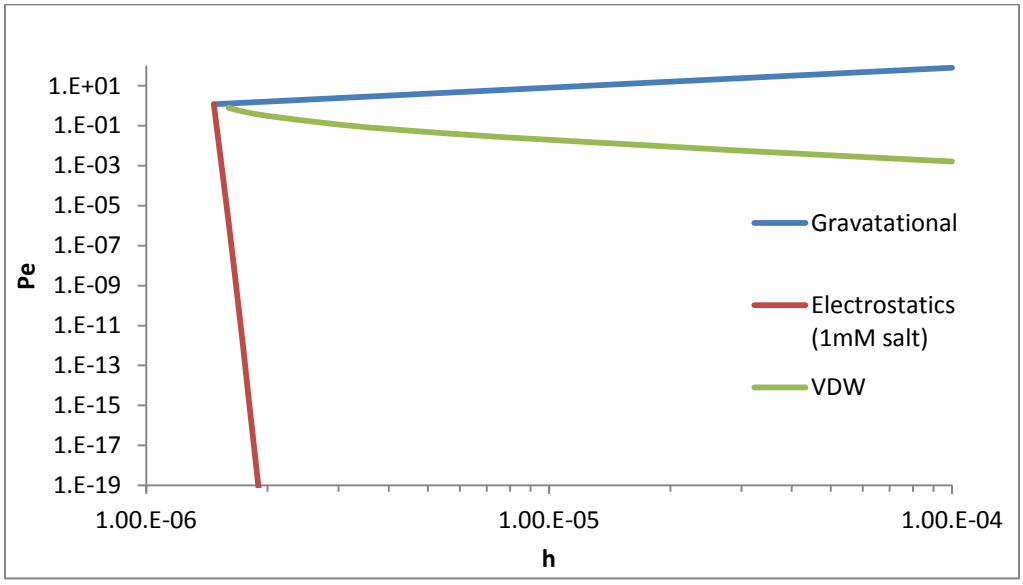

Figure 5: Comparison of Gravitational, Electrostatics, and Van der Waals Péclet Numbers

As seen in Figure 5, the Electrostatic Péclet number is high at low h values, but quickly declines to zero as h increases. Since the Debye length is only effective at a short distance from the particle, the quick decay of the Electrostatic Péclet is logical. In contrast to the Electrostatic Péclet, the Gravitational and Van der Waals Péclet numbers remain relatively constant.

This comparison of Péclet number can be used to determine how to address the electrostatic effects of the f-sand system, which will be further discussed in Chapter 5, the Results section.

Chapter 5

Results and Discussion

Results of Quantification

In our experiments, we quantified several different seed varieties. The first collection of seeds was from Chiang Mai, Thailand, weighing on average 0.1933g ± 0.0457g (Neal 2013) and harvested between January-April 2012. Our results suggest that shelled Chiang Mai seeds are composed of 1.21% ± 0.18% MOCP (Fig 6). Similarly, our total protein quantification results for Chiang Mai seeds show that 21.99% ± 3.31% of unshelled Moringa seed is protein (Fig 7). There is some significant spread between data, ranging from 9.5%-28.9%, which could be the result of natural variation or intrinsic variability in the purification and quantification process.

The second collection of seeds was green seeds also from Chiang Mai, Thailand. Besides the color difference between the green and brown Chaing Mai seeds, the green seeds were significantly smaller than the brown, weighing on average 0.0667g ± 0.0085g. The total protein measured 9.10% ± 2.83% and the MOCP was 0.651% ± 0.056%

The third collection of seeds was collected by Penn State student Cara Macdonald in 2013 from Arcahaie, Haiti from a small garden of trees. These seeds were brown but slightly larger than the brown Chiang Mai seeds at 0.2138g ± 0.0221g. The results of the protein assay showed total protein to be 10.22% ± 1.22% and MOCP to be 0.456% ± 0.064%.

The results for the total protein quantification and the MOCP quantification were complied and compared in Figures 6 and 7.

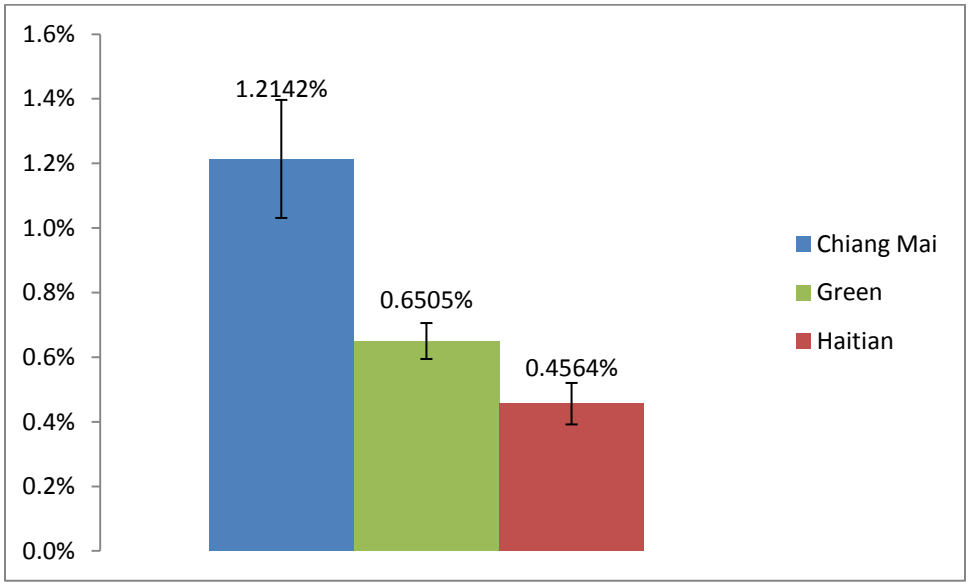

Figure 6: MOCP Quantification Results

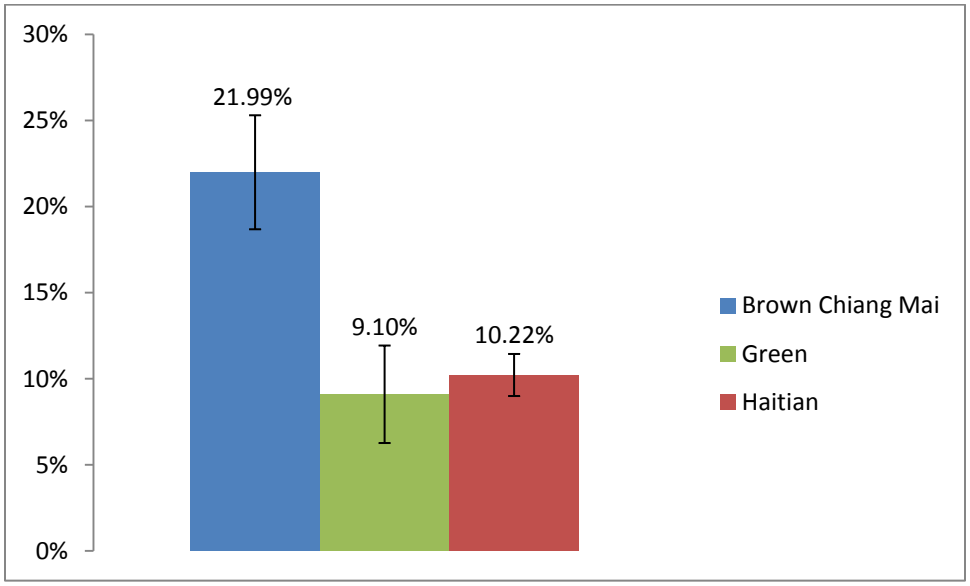

Figure 7: Total Protein Quantification Results

When interpreting the quantification of MOCP and total protein data, it is important to be aware of the limitations of this work. These seeds represent only a small sample of many

Moringa seeds. Most of these seeds were harvested in a span of weeks to months and were taken from a single tree, so a more diverse seed selection may be needed to make broader conclusions about MOCP content.

However from these results, it is clear that there is natural variation in MOCP content of Moringa seeds. It has long been suggested by anecdotal evidence that young green seeds are not as effective at purifying water as more mature seeds, and that may be due to the difference in MOCP content as seeds age. The higher MOCP concentration in brown seeds makes browns seeds a better choice to use in the creation of f-sand. Additionally, since the brown seeds are typically bigger than the green, the brown seed not only give more MOCP per gram, but more total MOCP per seed.

Furthermore, there is variation in MOCP levels between the mature Haiti and Indian seeds. This could indicate that Indian seeds are more MOCP dense than their Haitian counterparts, or it could be due to natural variation in MOCP levels among Moringa trees. MOCP quantification of seeds from additional trees from both countries would be needed to definitively tell. However, it is clear that MOCP concentration is not standard in all Moringa seeds. Like many living systems, there is a range of protein level in Moringa rather than a single value.

Results of Modeling

The Péclet numbers defined in Chapter 4 can be compared by looking at the distance h from the collector where they are comparable in magnitude. To accomplish this, the Electrostatics Péclet number and Gravitational Péclet number can be set equal to each other and

solved for the h^* value in which they are equal. Essentially, we are defining a new dimensionless constant that relates the effect of gravity to the effect of electrostatics.

$$Pe_g = Pe_{es} \quad \textbf{Eq 44}$$

$$\frac{\frac{2}{3}\pi a^3(\rho_p - \rho_f)gh^*}{kT} = \frac{\pi\varepsilon_0\varepsilon_r a\zeta_p\zeta_w e^{(a-2h^*)\kappa}(-1 + e^{h^*\kappa} - h^*\kappa)}{kTh^*\kappa} \quad \textbf{Eq 44}$$

$$h^* = \frac{2\text{ProductLog}\left[-\frac{i\sqrt{\frac{3}{2}}e^{\frac{a\kappa}{2}}\sqrt{\varepsilon_0\varepsilon_r\zeta_p\zeta_w\kappa}}{2a\sqrt{g\rho}}\right]}{\kappa}, h^* = \frac{2\text{ProductLog}\left[\frac{i\sqrt{\frac{3}{2}}e^{\frac{a\kappa}{2}}\sqrt{\varepsilon_0\varepsilon_r\zeta_p\zeta_w\kappa}}{2a\sqrt{g\rho}}\right]}{\kappa} \quad \textbf{Eq 46}$$

This value of h^* was found through the use of the computational software Mathematica. This solution is in the form of a Lambert W-function, the inverse function of $f(W) = We^W$ that is often abbreviated as "Product log". Although the function is in the complex plane, it gives real answers.

h^* can be added to the collector radius, a_c, to create an "effective radius" of the collector, meaning that the effect of electrostatics makes the collector particle slightly larger than it actually is. By selecting a value for the collector radius, a_c, a sample calculation can be completed for h^* for any contaminant particle of diameter "a". Consistent with Table 2, a_c=115μm.

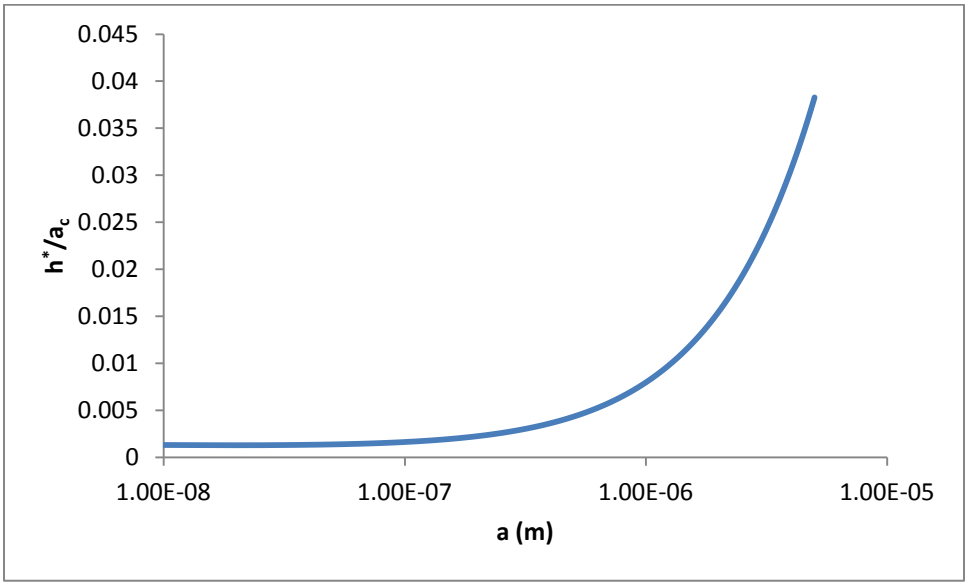

Figure 8: Particle Radius, a vs. Fraction Increase in Collector Radius, h^*/a_c

Although the true radius of the collector will be used in all η calculations, h^* can be used to define a new value for porosity, Θ^*.

$$\theta^* = \frac{\frac{4}{3}n\pi(h^* + a_c)^3}{V} \quad \textbf{Eq 47}$$

where n is the number of total collectors and V is the volume of the column. Since calculating the number of collectors proves difficult, the effective porosity can be related back to the experimentally measured porosity Θ.

$$\frac{1-\theta^*}{1-\theta} = \frac{\left(\frac{4n\pi(a_c + h^*)^3}{3V}\right)}{\left(\frac{4n\pi a_c^3}{3V}\right)} \quad \textbf{Eq 48}$$

Canceling like terms, and solving for Θ^* results in:

$$\theta^* = 1 - \frac{(a_c + h^*[a])^3}{a_c^3} + \frac{(a_c + h^*[a])^3}{a_c^3}\theta \quad \textbf{Eq 49}$$

where h* is a function of the contaminant particle radius, a.

Using Equation 49, a Θ^* can be defined for the f-sand system shown in Table 2, where a_c=115μm and a=1.45μm. At this value of a, h^*=1.47μm.

$$\theta^* = 1 - \frac{(115\mu m + 1.47\mu m)^3}{115\mu m^3} + \frac{(115\mu m + 1.47\mu m)^3}{115\mu m^3}(0.36) = 0.335 \quad \textbf{Eq 50}$$

This modified Θ^* can be used to calculate a new collector efficiency η, similar to the calculation in Chapter 4, Section "Applying the RT Model to the F-sand System." The new η^* equals 0.0210, which is statistically different from the η=0.0180 calculated with the new porosity. The difference between these two theoretical calculated η's is shown alongside the experimentally determined η in Figure 9.

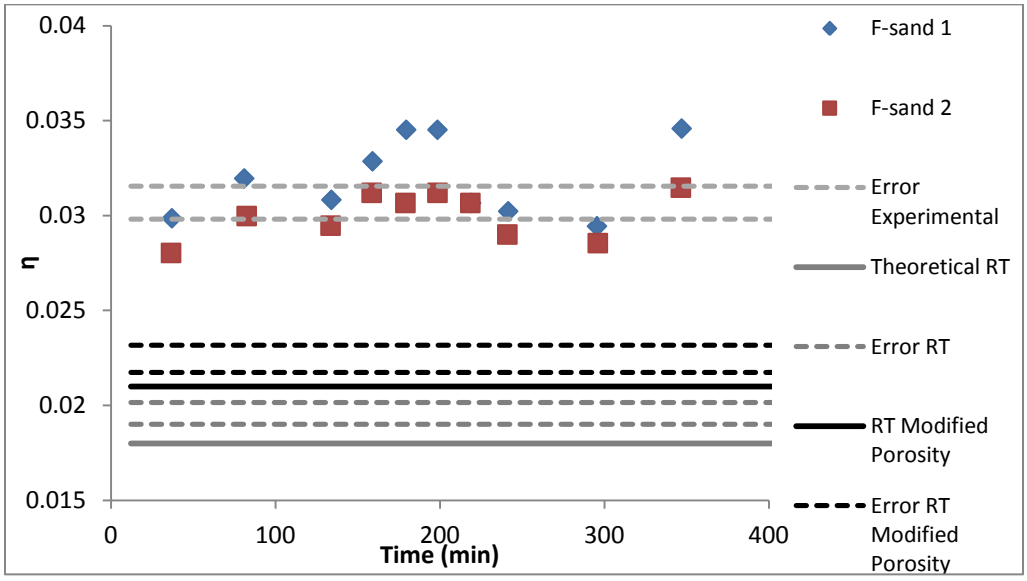

Figure 9: Comparison of Theoretical and Experimental Data with Modified Porosity

Clearly, with this effective porosity, the modified η is slightly closer to matching the experimental results. This is a demonstration of one way to adjust the RT model based on the experimental system; alternative ways will be discussed in Chapter 6.

Chapter 6

Conclusions and Future Work

Protein Quantification Conclusions and Future Work

Brown seeds from Chiang Mai, Thailand were found to have a total protein content of 21.99% ± 5.85% and an MOCP content of 1.21% ± 0.18%. Green seeds from the same area had less total protein at 9.10% ± 2.83% and less MOCP 0.651% ±0.056% than their more mature counterparts. Additionally, seeds from Arcahaie, Haiti contained total protein 10.22% ± 1.22% and MOCP 0.456 ± 0.064%. Future work could involve quantifying protein from additional Moringa tree seeds from both Chiang Mai and Arcahaie to make further conclusions on these trends. Moreover, Moringa seeds from other equatorial areas could be quantified with this procedure.

The development of a batch method to purify and quantify MOCP is a new process, and allows researchers to calculate the concentration of MOCP in Moringa seeds. Before this research, the amount of MOCP remained undetermined. This method is especially useful for comparing different types of seeds and predicting their purification potential. Future work could involve switching from a batch method to a continuous method (Shebeck 2015) of protein purification, which could be less time-consuming and ultimately yield more protein.

Conclusions on the F-Sand Modeling

To begin modeling the f-sand system, the RT model was used at the parameters shown in the table below.

Table 3: Input Parameters for the F-sand Column

Input Parameters	Example Value	Units	Typical Ranges
T	298 ± 10	K	273-310K
d_p, particle diameter	2.90E-6 ± 8.99E-8	m	10-8-10-5m
d_c, collector diameter	2.10E-4 ± 2E-5	m	10-4-10-3m
Q, flow rate (vA)	1.05E-8 ± 1.05E-9	m^3/s	----------
D, Diameter of the column	0.01 ± 0.001	m	----------
ρ_p, Density of particle	1050 ± 2.89	kg/m^3	----------
Θ, porosity	0.36 ± 0.036		0.25-0.70
A, Hamaker constant	1.4E-20 ± 1.41E-21	J	10^{-21}-10^{-19}J
L, Length	0.1 ± 0.01	m	----------

An η can be calculated based on the values in Table 3, which can be compared to an experimental η. The experimental η was determined by data collected under the same conditions shown in Table 3 and with the assumption of "perfect collector stickiness" or α=1. The theoretically determined η from the RT model was η=0.0180 and the experimentally determined η is η=0.0307 ± 0.0009. These η's were determined to be statistically different, so using a theoretically calculated η and assuming α=1 for laboratory experiments does not aptly predict the experimental conditions.

Another way to use the RT model in the creation of a model for f-sand is to use the theoretical η value, η=0.0180, and experimental data for N/N_0 to calculate a value of α. For these parameters, a value of α=1.705 ± 0.044 was obtained. Values of α greater than 1 have no direct physical interpretation; however, it is feasible to use these non-realistic α values to model experimental conditions.

One reason for the discrepancy between the RT model prediction and the f-sand experimental data could be the omission of electrostatic effects in the RT model. To model f-sand's electrostatic interactions and assess their relative importance, Péclet numbers were defined for Van der Waals, gravitational and electrostatic forces. By setting the Electrostatics Péclet number equal to the Gravitational Péclet number, the distance between the collector and contaminant particle over which electrostatic interactions are most relevant, h^*, can be determined.

The value of h^* can be used to calculated a modified porosity value that accounts for the electrostatic effect of f-sand. For the current f-sand experiment, the modified porosity values is Θ^*=0.335, lowered from the original porosity value of Θ=0.36. Using the modified porosity value, a new η of η=0.0210 was determined. Although that is still not the same as the experimental η value, this modification to the model is a step in the right direction.

Modeling Future Work

This work represents the first attempt at modeling the particle removal of the f-sand column, so there is still a significant amount of work to be done. First, a larger amount of experimental data is needed to compare against the model predictions. Only two experiments

were run at the conditions shown in Table 3, so more are needed to limit experimental error. Further, other experimental conditions such as different particle sizes, column scales, and collector types must be tested and subsequently modeled. It is important to make a model that not only works for one scenario, but for a variety of experimental conditions.

The RT model used for modeling particle removal is a clean-bed filtration model, meaning that it assumes that there is no build-up of contaminant particles on the collector surface. While this assumption is valid for the start of filtration, it begins to fail over time as contaminant particle build-up, called blocking, is more prevalent. Using a model that incorporates blocking will allow the f-sand model to predict over a longer time scale.

Also, further work should be completed on the modified porosity version of the RT model. Setting the Gravitational and Electrostatics Péclet numbers equal to each other was a somewhat arbitrary choice in order to find an h^* at which the electrostatic and gravitational forces were comparable in magnitude. These Péclet numbers need not be in a 1:1 ratio; a different ratio can be selected to better match experimental data. Another option could be to set the Electrostatics Péclet equal to the Van der Waals Péclet to see if that yields a closer match between the model and experimental data.

Additionally, other models for particle removal can be explored to better model f-sand. In this work, the RT model was used as the base model and adapted to fit the f-sand column, but the RT model may not be the best match for this system. Specifically, the Elimelech model for particle removal has been shown to be an improvement on the RT model (Logan 2012), and therefore should be investigated for f-sand modeling.

Appendix A
Moringa Protein Purification and Quantification Protocol

Preparation of Moringa seeds

1. Choose ~10 random seeds from Chiang Mai bag (or other variety of Moringa seed).
2. Shell seeds.
3. Grind seeds with coffee grinder until a fine powder. (Takes approximately 5 minutes).
4. Store in a plastic Petri dish with a cover at room temperature.

Solubilization of protein from seeds.

5. Weigh out 0.1 g of seed.
6. Add it to 10 mL of DI water.
7. Mix for 1 hour on stir plate, longer mixing is also fine.
8. Filter through 5 μm filter paper (wet paper first with DI), then filter through 0.2 μm syringe filter. (Final volume ≈ 8-8.5 mL) This is the MOS bulk solution. (bulk seed mixture = 100 mg/8 mL)

Quantification of total protein

9. Start water bath to 37 C.
10. Prepare working reagent. The ratio of working reagent A should be in a relationship of 50 to 1. For example, for 40 samples, add 14.71 mL of A and 0.29 mL of B. Mix it on a vortex mixer for 10 seconds. It should be a green solution with no precipitation in the solution.
11. Preparing 9 BSA standards from 0 – 2000 μg/mL. Store these standards in the fridge.
12. Use a micropipette to measure out 10 μL of the MOS bulk solution into an Eppendorf tube. Repeat 2 more times.
13. Add 10 μL of DI water to the 10 μL of MO bulk solution. Mix. This the MOS dilute solution (should be around 1 mg/mL).
14. Add 200 μL of the working reagent to the 10 μL of the MOS dilute bulk solution. Repeat 2 more times. (3 total samples)
15. Add 200 μL of the working reagent to each of the nine 10 μL of each BSA standard. Repeat 2 more times. (27 total standards)

16. Incubate in the water bath at 37 C for 30 minutes. (The tubes are in test tube tray). Sample color will range from green (no protein) to clear (a little bit of protein) to purple (some protein).
17. Use a micropipette to measure 200 μL into each well of a 96 microplate.
18. Put microplate in plate reader (Use Plate reader located in Millennium Science or Sackett Building)
19. Measure absorbance at 562 nm.

Analyze data

20. Subtract the Absorbance of standard 9 from all the other standards within that set of standards.
21. Find the average absorbance for standard 1 – 9.
22. Plot Concentration vs. Abs for standards 1 - 9. Fit it to a polynomial fit with degree 2. Set intercept to zero.
23. Average the 3 points for standard 9. Subtract this value from each of your absorbance values of the samples.
24. Use the polynomial equation to calculate concentration from the new absorbance of your sample.
25. Adjust for dilution.

Purification of MOCP

26. Hydrate the spin columns. 0.2 mL of DI water to each column. Let it sit for 30 minutes – 60 minutes.
27. Centrifuge spin columns once to remove DI water. (2000 g **for 2 minutes)**
28. Add 0.2 mL of the bulk seed solution to the spin column.
29. Centrifuge at 2000 g for 2 minutes.
30. Pipette 0.2 mL from bottom of tube back into the spin column. Centrifuge again.
31. Discard eluent.
32. Add another 0.2 mL of MOS to spin column. Centrifuge. Reload it again. Centrifuge again.
33. Discard eluent.
34. Add 0.2 mL of DI water to spin column. Centrifuge. Discard eluent.
35. Repeat steps until you have double loaded 3 mL of MOS bulk solution. (If we assume 1% MOCP, 3 mL/10 mL x 0.1 g seed = 0.03 g MOS is on the column.)

36. Add 0.2 mL of 200 mM NaCl to spin column. Centrifuge. (Keep eluent – do an SDS page to determine proteins coming off.)
37. Add 0.2 mL of 600 mM NaCl to spin column. Centrifuge. Keep eluent. Repeat 15 times until you have 3 mL of solution. This is the MOCP solution.
38. Add 3 mL of MOS solution to 3000 Da centrifuge filter. Centrifuge this at 700 g for 7 minutes. This removes anything below 3000 Da. You now have 0.5 mL of MOCP (still have 0.3 mg of MOCP).
39. Take 0.5 mL of MOCP and add to a dialysis cassette. MW cut off is 3500 Da. Add dialysis cassette to 300 mL PBS buffer with 150 mM NaCl.
40. Remove solution from dialysis cassette with a pipette. Weigh in a tared Eppendorf tube. (0.03 mg/0.5 mL = 0.06 mg/mL)

Quantification of Cationic Protein

(Same procedure as total protein quantification)

41. Start water bath to 37 C.
42. Prepare working reagent. The ratio of working reagent A should be in a relationship of 50 to 1. For example, for 40 samples, add 14.71 mL of A and 0.29 mL of B. Mix it on a vortex mixer for 10 seconds. It should be a green solution with no precipitation in the solution.
43. Preparing 9 BSA standards from 0 – 2000 μg/mL. Store these standards in the fridge.
44. Use a micropipette to measure out 10 μL of the MOCP bulk solution into an Eppendorf tube. Repeat 2 more times.
45. Add 200 μL of the working reagent to the 10 μL of the MOCP dilute bulk solution. Repeat 2 more times. (3 total samples)
46. Add 200 μL of the working reagent to each of the nine 10 μL of each BSA standard. Repeat 2 more times. (54 total standards)
47. Incubate in the water bath at 37 C for 30 minutes. (The tubes are in test tube tray). Sample color will range from green (no protein) to clear (a little bit of protein) to purple (some protein).
48. Use a micropipette to measure 200 μL into each well of a 96 microplate.
49. Put microplate in plate reader (Use Plate reader located in Millennium Science or Sackett Building)
50. Measure absorbance at 562 nm.

Data Analysis of Quantification Results

51. Subtract the Absorbance of standard 9 from all the other standards within that set of standards.
52. Find the average absorbance for standard 1 – 9.
53. Plot Concentration vs. Abs for standards 1 - 9. Do this for each set of standards. Fit it to a polynomial fit with degree 2. Set intercept to zero.
54. Average the 3 points for standard 9. Subtract this value from each of your absorbance values of the samples.
55. Use the polynomial equation to calculate concentration from the new absorbance of your sample.

Appendix B
Example Standards Data and Graph

Table 4: Example Standards Data

Concentration	**Abs 1**	**Abs 2**	**Abs 3**	**Ave**	Ave-Zero Point
2000	1.989	1.598	1.695	**1.761**	1.61
1500	1.159	1.402	1.343	**1.301**	1.15
1000	1.025	0.957	0.605	**0.991**	0.84
750	0.829	0.817	0.666	**0.771**	0.62
500	0.533	0.589	0.601	**0.574**	0.42
250	0.353	0.401	0.418	**0.391**	0.24
125	0.255	0.276	0.269	**0.267**	0.11
25	0.172	0.185	0.194	**0.184**	0.03
0	0.152	0.143	0.166	**0.154**	0.00

Shown in yellow in Table 4 is the raw absorbance data from the plate reader. This data is averaged, and the absorbance at a concentration of zero is subtracted from each data point. The data is then graphed. A quadratic fit is typically used, although oftentimes a linear fit works well, especially for the lower range absorbance values. The intercept is set at (0,0) and the R^2 value is typically greater than 0.99.

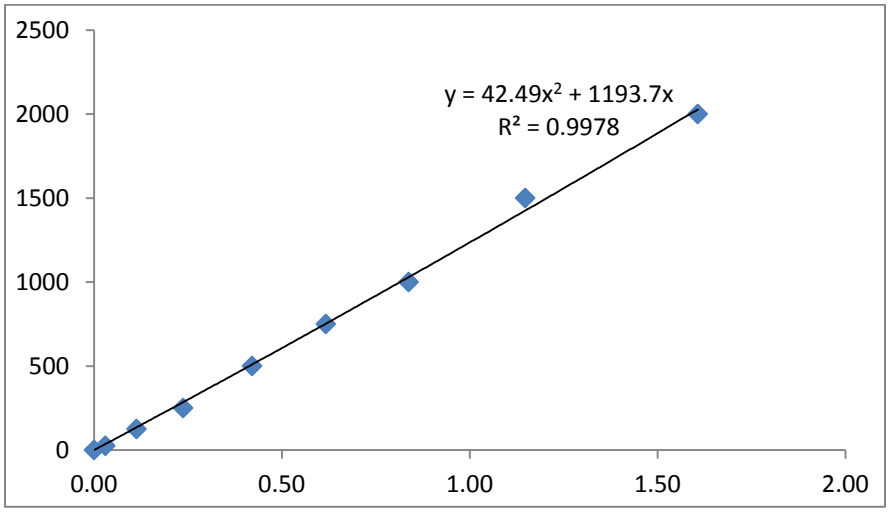

Figure 10: Sample Standards Graph

There is some variance between standards from different quantifications. Therefore, it is important to test new standards for each quantification of Moringa protein. Shown below are a few examples of standards graphs and how they vary.

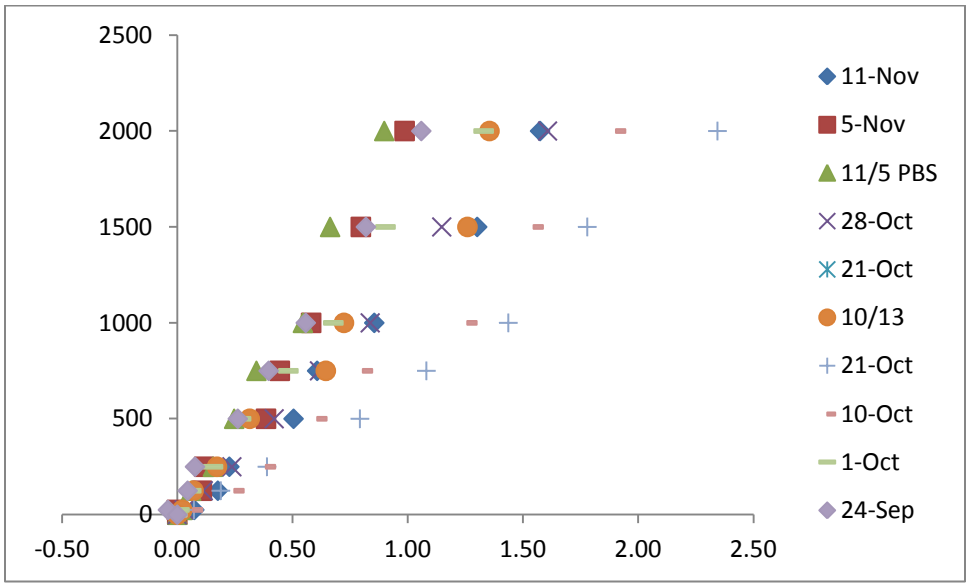

Table 5: Comparison of Standards Data

Appendix C
Results of Chiang Mai Brown Seeds Quantification Experiment

Table 6: MOCP Quantification of Brown Chiang Mai Seeds

Trial Number	Percent MOCP
1	1.61%
2	0.89%
3	1.18%
4	0.84%
5	1.23%
6	1.64%
7	1.34%
8	1.05%
9	1.14%
Average	1.21%
Standard Deviation	0.27%
95% Confidence	0.18%

Table 7: Total Protein Quantification of Brown Chiang Mai Seeds

Trial	Total Protein Percentage
1	27.42%
2	25.29%
3	28.90%
4	21.52%
5	26.31%
6	27.32%
7	12.59%
8	27.74%
9	19.20%
10	17.12%
11	9.52%
12	20.89%
Average	21.99%
Standard Deviation	5.85%
95% Confidence	3.31%

References

Gassenschmidt, U.; Jany, K. D.; Tauscher, B.; Niebergall, H., Isolation and Characterization of a Flocculating Protein from Moringa-Oleifera Lam. *Bba-Gen Subjects* **1995**, 1243, (3), 477-481.

Hoefer Inc. Macro SpinColumns, Ion Exchange. Digital image. Hoefer. 4 Apr. 2015.

Jerri, H., K. Adolfson, L. McCullough, D. Velegol, S. Velegol. Antimicrobial Sand via Adsorption of Cationic *Moringa oleifera* Protein. *Langmuir* **2012**, 28(4), 2262-2268

Logan, B. *Environmental Transport Processes* **1999**, Ed. 1, 564-604.

Logan, B. *Environmental Transport Processes* **2002**, Ed. 2, 408-432.

Ndabigengesere, A.; Narasiah, K. S.; Talbot, B. G. Active agents and mechanism of coagulation of turbid waters using Moringa Oleifera. *Water Res* **1995**, 29(2), 703–710.

Neal, A. Turbidity Removal from Kaolin Suspensions and Wastewater using *Moringa Oliefera*. Schreyer Honors College **2013.**

Paramonova, E.; Zerfoss, E.; Logan, B. Measurement of Biocolloid Collision Efficiencies for Granular Activated Carbon by Use of a Two-Layer Filtration Model. *Applied and Environmental Microbiology* **2006**, 72 (8). 5190-5190.

Rajagopalan, R.; Tien C. Trajectory analysis of deep-bed filtration with the sphere-in-a cell porous media model. *AIChE J* **1976**, 22(3), 523-533.

Shebeck, K.; Schantz, A.; Sines; I., Lauser, K.; Velegol, S.; Kumar, M. (in press). The flocculating cationic polypeptide from *Moringa oleifera* seeds damages bacterial cell membranes by causing membrane fusion. *Langmuir* **2015**.

Suarez, M.; Haenni, M.; Canarelli, S.; Fisch, F.; Chodanowski, P.; Servis, C.; Michielin, O.; Freitag, R.; Moreillon, P.; Mermod, N., Structure-function characterization and optimization of a plant-derived antibacterial peptide. *Antimicrobial Agents Ch* **2005**, 49, (9), 3847-3857.

Uliana, Adam. Personal Correspondence. 2014.

Velegol, D. (in press). *Colloidal Systems* **2012**, 6.

Yao, K.; Habibian, M. T.; O'melia, C.R. Water and wastewater filtration: concepts and applications. *Envir. Sci.Technol.* **1971**, 5(11), 1105-112.

ACADEMIC **VITA**

Kathleen Lauser
Kathleen.lauser2@gmail.com

EDUCATION:

The Pennsylvania State University, Schreyer Honors College May 2015
Bachelor of Science in Chemical Engineering
Minors in Mathematics and in Environmental Engineering
Honors in Environmental Engineering

WORK EXPERIENCE:

Bristol-Myers Squibb Chemical Development Intern Summer 2014
Bristol-Myers Squibb R&D, New Brunswick, NJ
- Characterized mixing in a lab reactor using the 4th Bourne Reaction
- Modeled lab and pilot plant reactor mixing using CFD and compared with lab results
- Validated experimental workflow with a BMS portfolio project

NIST Fire Research Intern Summer 2013
National Institute of Standards and Technology, Gaithersburg, MD
- Studied Wildland Urban Interface (WUI) fires and their ignition
- Characterized embers from NIST Dragon using imaging software
- Presented findings in presentation to NIST scientists and written report to Department of Homeland Security

Learning Edge Academic Program (LEAP) Mentor Summer 2012
The Pennsylvania State University, University Park, PA
- Promoted academic and social transitions for 24 first-year engineering students
- Successfully incorporated an additional 17 students into the LEAP group

RESEARCH EXPERIENCE:

Moringa Undergraduate Researcher 2013-2015
The Pennsylvania State University, University Park, PA
- Researched *Moringa oleifera* seed to develop sustainable water purifications system for developing countries
- Quantified the cationic protein in Moringa seed as a metric for seed comparison
- Formulated a model for particle removal of an f-sand filter

Chemical Engineering Undergraduate Researcher 2012-13
The Pennsylvania State University, University Park, PA
- Prepared algae growth media and subcultures for biofuel research
- Maintained cynobacteria cultures for pH experimentation

LEADERSHIP AND INVOLVEMENT:

Tutor and Member, Chemical Engineering Honors Society OXE 2013-15
Mentor, Penn State Women in Engineering Program Orientation 2013-15
Member, American Institute of Chemical Engineers (AIChE) 2012-15

HONORS

Dean's List 2011-15
Recipient, Schreyer Honors College Scholarship 2011-15
Recipient, Siemens Corporation National Merit Scholarship 2011-15